HHS Public Access

Author manuscript

Cancer Lett. Author manuscript; available in PMC 2021 October 27.

Published in final edited form as:

Cancer Lett. 2016 December 28; 383(2): 161–170. doi:10.1016/j.canlet.2016.09.005.

Lgr4 is crucial for skin carcinogenesis by regulating MEK/ERK and Wnt/β-catenin signaling pathways

Peng Xu[a,1], **Yongyan Dang**[a,1], **Luyang Wang**[a], **Xia Liu**[a], **Xiaolin Ren**[a], **Jun Gu**[b], **Mingyao Liu**[a], **Xing Dai**[c,**], **Xiyun Ye**[a,*]

[a]Shanghai Key Laboratory of Regulatory Biology, Institute of Biomedical Science and School of Life Science, East China Normal University, Shanghai 200241, China

[b]Department of Dermatology, Changhai Hospital, Second Military Medical University, 168 Changhai Road, Shanghai 200433, China

[c]Department of Biological Chemistry, University of California, D250 Med Sci I, Irvine, CA 92697-1700, USA

Abstract

Lgr4 is a member of the leucine-rich, G protein–coupled receptor family of proteins, and has recently been shown to augment Wnt/β-catenin signaling via binding to Wnt agonists R-spondins. It plays an important role in skin development, but its involvement in skin tumorigenesis is unclear. Here, we report that mice deficient for Lgr4 are resistant to 12-O-tetradecanoyl-phorbol-13-acetate (TPA)-induced keratinocyte proliferation and papilloma formation. We show that TPA treatment activates MEK1, ERK1/2 and downstream effector AP-1 in wild-type (WT) epidermal cells and mice, but not in cells or mice where Lgr4 is depleted. Wnt/β-catenin signaling is also dramatically activated by TPA treatment, and this activation is abolished when *Lgr4* is deleted. We provide evidences that blocking both MEK1/ERK1/2 and Wnt/β-catenin pathways prevents TPA-induced increase in the expression of *Ccnd1* (cyclin D1), a known Wnt/β-catenin target gene, and that the activation of MEK1/ERK1/2 pathway lies upstream of Wnt/β-catenin signal pathway. Collectively, our findings identify Lgr4 as a critical positive factor for skin tumorigenesis by mediating the activation of MEK1/ERK1/2 and Wnt/β-catenin pathways.

Keywords

Lgr4; Squamous cell carcinoma; TPA; ERK1/2; β-Catenin

*Corresponding author. East China Normal University, 500 Dongchuan Road, Shanghai 200241, China. xyye@bio.ecnu.edu.cn (X. Ye). **Corresponding author. xdai@uci.edu (X. Dai).

[1]The two authors contributed equally to this work.

Conflict of interest

None.

Appendix A. Supplementary data

Supplementary data related to this article can be found at http://dx.doi.org/10.1016/j.canlet.2016.09.005.

Introduction

Lgr4, also known as Gpr48, belongs to the leucine-rich, G protein–coupled receptor (GPCR) family. Lgr4 is known to be important for the development of the male reproductive tract, eyelids, hair and bone [1–4]. Lgr4-deficient mice show marked intrauterine growth retardation coupled with embryonic and perinatal lethality [5]. A role for Lgr4 in tumor formation and metastasis has also been suggested. It promotes prostate tumorigenesis via PI3K/Akt signaling pathway [6] and accelerates metastasis of colorectal cancer cells [7]. However, the function of Lgr4 in skin cancer development has not been well investigated.

Squamous cell carcinoma (SCC) is the second most common skin cancer in humans. The molecular mechanisms of SCC remain to be fully understood. The mitogen activated protein kinase (MAPK) pathway has been implicated in skin cancer development. In the ERK signaling pathway, ERK1 or ERK2 (ERK1/2) is activated by MEK1/2, which in turn is activated by Raf [8]. Mice lacking epidermal MEK1 protein develop fewer papillomas than the WT controls following 7,12-Dimethylbenz[a]anthracene (DMBA)/TPA treatment [9]. ERK activation results in the elevated activity of the AP-1 transcriptional complex, which is composed of c-Jun and c-Fos proteins that are known positive regulators of cell proliferation and transformation [10]. The B-RAF/MEK/ERK MAP kinase pathway is reported to be a target for all-trans retinoic acid during skin cancer promotion [11]. However, the precise mechanism by which MAPK signal pathway facilitates skin cancer development remains elusive.

There is also mounting evidence that Wnt/β-catenin signaling is involved in the formation of skin cancers. Canonical Wnt signaling activates a series of intracellular events culminating in the stabilization and nuclear translocation of β-catenin, which complexes with TCF/TCF factors to regulate gene expression [12]. The β-catenin/TCF pathway is constitutively activated in non-melanocytic skin tumors induced by a two-stage chemical carcinogenesis protocol [13]. Long-term exposure of mice to ultraviolet B (UVB) irradiation results in upregulation of β-catenin, contributing to skin carcinogenesis [14]. In addition, Wnt/β-catenin signaling plays a critical role in the maintenance of skin cancer stem cells in epidermal tumors [15].

Recent studies have uncovered an intimate molecular relationship between Lgr4 and Wnt/β-catenin signaling. Lgr4 and its homologues, Lgr5 and Lgr6, have been shown to act as facultative Wnt receptor components that bind soluble R-spondin proteins to facilitate Wnt signaling enhancement [16]. Depletion of Lgr4 completely abolishes RSPO-induced β-catenin signaling in HEK293T cells [17]. In colorectal cancer, Lgr4 increases nuclear β-catenin accumulation and expression of Wnt target genes such as cyclin D1 and c-Myc [18]. Lgr4 is essential for spermatogenesis through mediating Wnt/β-catenin signaling in peritubularmyoid cells [19]. Lgr4 also regulates mammary development via the Wnt/β-catenin/Lef1 pathway [20]. In addition, Lgr4 is critically involved in the maintenance of intestinal homeostasis and protection against inflammatory bowel disease through modulation of the Wnt/β-catenin signaling pathway [21]. Thus, Lgr4 is a positive regulator of Wnt/β-catenin signaling in a number of cell/tissue contexts. However, it is still

unclear whether Lgr4 plays a role in regulating Wnt/β-catenin signaling during skin cancer development.

In the present study, we report that Lgr4 promotes skin tumor development in a two-stage skin carcinogenesis mouse model. Lgr4 is required for the maximal activation of MEK/ERK and Wnt/β-catenin signaling pathways in TPA-induced skin tumors. Activation of the MEK/ERK pathway further enhances Wnt/β-catenin signaling. Thus, TPA stimulation augments the facilitative effects of Lgr4 on β-catenin activation, leading to abnormal keratinocyte proliferation and papilloma formation.

Materials and methods

Mice

Lgr4$^{-/-}$ mice were generated as previously described (Weng et al., 2008). Mice were provided with food and water ad libitum, and were housed under standard conditions, with a constant temperature and a 12-h light/dark cycle. All experiments were approved by the Animal Care and Use Committee of East China Normal University.

Skin chemical carcinogenesis

All animal experiments were performed with 8-week-oldWT and *Lgr4* KO mice. Each experimental group consists of 12 female and 12 male mice. Mice were shaved, followed by application of a single dose of 50 μg of 7,12-Dimethylbenz[a]anthracene (DMBA) (Sigma) in 200 μl acetone. A week later, 10 μg of TPA (Sigma) in 200 μl acetone was applied twice weekly to the shaved back skin for 20 weeks. Skin tumors were counted every week. The multiplicity and incidence of papillomas, which were expressed as the average number of tumor per surviving mouse and the percentage of tumor-bearing mice, respectively, were calculated each time when tumors were counted.

For the short-term TPA experiments, 10 μg of TPA in 200 μl acetone was applied to the shaved dorsal skin of WT (n = 3) and KO (n = 3) littermates every other day over two weeks. Mice were sacrificed and skin samples were collected 24 h after the last treatment.

Cell culture, plasmids and stable transfection

A431 human epidermoid carcinoma cells were cultured in Dulbecco's Modified Eagle's Medium (DMEM; Gibco) supplemented with 10% fetal bovine serum (FBS). To stably knockdown *Lgr4*, double-stranded oligonucleotides encoding shRNA against mouse *Lgr4* were inserted into the pLKO.1-U6-TRC vector (Addgene). A pLKO.1-U6-TRC-unrelated sequence vector was used as control. Transfection was carried out with Lipofectamine 2000 (Invitrogen) according to manufacturer's instructions. Clones with stable integration of the target plasmid were selected by puromycin treatment (0.3 μg/ml) for a month. Positive clones were verified by decreased *Lgr4* expression. The siRNA sequences were as follows: 5′-CCGGGCGTAATCAAATCTACCAAATCTCGAGATTTGGTAGATTTGATTACGCTTTTT-3′. A431 cells were treated with 100 ng/ml of TPA or acetone for 4 h for subsequent analysis.

Primary keratinocyte culture

Primary keratinocytes were isolated from the tail skin of adult mice using dispase II (Sigma) and cultured in 154CF medium supplemented with human keratinocyte growth supplement (HKGS), 0.2 mM $CaCl_2$ and Pen Strep (100 units/ml Penicillin and 100 μg/ml Streptomycin) (Invitrogen, Shanghai). Keratinocytes were seeded in six-well plates and incubated at 37 °C in 5% CO_2. Cells were treated with 200 ng/ml of TPA or acetone for 4 h for subsequent analysis.

For ERK knockdown, cells were infected with lentiviral particles that express short hairpin RNA (shRNA) against ERK1 and ERK2 for 24 h. The shRNA sequences were as follows: ERK1, 5′-CCATGAGAATGTTATAGGCAT-3′; ERK2, 5′-GCTGAATCACATCCTGGGTAT-3′.

Cell proliferation and colony formation assay

A431 cells were plated in 6-well plates at a seeding density of $1 \times 10^5/10$ cm^2 in triplicate. Each day, cells were harvested by trypsinization, and cell numbers were determined using a hemocytometer. For colony formation assay, cells were plated at the same seeding density in 6-well plates in triplicates, and cultures were allowed to grow for 15 days. The colonies were fixed in 2% paraformaldehyde for 30 min, and then stained with crystal violet (0.4 g/L; Sigma) for 30 s followed by washing extensively to remove excess dye.

MTS assay

A431 cells were plated in 96-well plates at 2×10^4/well. The cells were further incubated in DMEM for 24, 48 and 72 h, respectively. After a brief wash with medium, 3-(4,5-dimethylthiazol-2-yl)-5-(3-carboxymethoxyphenyl)-2-(4-sulfophenyl)-2H-tetrazolium (MTS) (0.5 mg/ml in DMEM) was used for the quantification of metabolically active cells. Mitochondrial dehydrogenases metabolized MTS to a brown soluble formazan dye, which was measured photometrically at 490 nm.

Flow cytometric analysis for cell cycle

A431 cells (1×10^6) were trypsinized and washed in ice-cold PBS. Cells were then fixed with 70% ethanol for 12 h at 4 °C. After washing, cells were resuspended and incubated at 37 °C for 30 min in 0.5 ml of PBS containing 10 μg/ml propidium iodine (Sigma) and 5 μg/ml RNase A (Sigma). Proportions of cells in G1 or S phase of cell cycle were analyzed by flow cytometry (FACSCalibur, BECTON–DICKINSON, USA).

Immunofluorescence analysis

A431 cells were fixed with 4% paraformaldehyde for 10 min after washing with PBS twice and permeabilized with 0.1% Triton X-100 for 10 min. After blocking with 0.2% BSA for 30 min, cells were incubated with the primary antibody against β-catenin (1:200; Cell Signaling Technology) overnight at 4 °C. Then, cells were incubated for 2 h at room temperature in the dark using the secondary antibody conjugated to FITC. Fluorescent images were observed by an Olympus fluorescence microscope (Olympus, Japan).

Histology and immunohistochemistry

The mouse normal skin, papillomas, human normal skin and human skin tumor samples were fixed by 4% paraformaldehyde and embedded in paraffin. Sections (5-μm thick) of tissue were cut, mounted on glass slides, and stained with haematoxylin-eosin (H&E). For immunostaining, slides were heated in a microwave oven in 0.01 mol/L citrate buffer (pH, 6.0) for 10 min at 95 °C, followed by rinsing with 1 × PBS. To eliminate endogenous peroxidases, slides were incubated in 3% hydrogen peroxide, and then incubated with 5% bovine serum albumin solution for 10 min. Slides were incubated with primary antibodies overnight at 4 °C, and staining accomplished using a horseradish peroxidase-diaminobenzidine (HRP-DAB) staining kit following manufacturer's instructions (M. R. Biotech). Primary antibodies used were: rabbit anti-PCNA (1:1000, Abcam), rabbit anti-Lgr4 (1:200, Abcam) and rabbit anti-Ki67 (1:1000, CST). Hematoxylin was used as a counterstain. Images were acquired by a LEICA DM-4000B fluorescent microscope (Leica Microsystems, Bannockburn, IL) with a Diagnostic RT-KE 2 MP digital camera (Diagnostic Instruments, Sterling Heights, MI) attached.

Western blot analysis and fractionation

Skin was lysed in RIPA buffer (50 mM Tris-Cl, pH 8.0, 150 mM NaCl, 1% Triton x-100, 1% Sodium deoxycholate, 0.1% SDS) on ice for 15 min after homogenizing. The lysates were run on a 10% SDS-polyacrylamide gel, and proteins transferred onto NC membranes. The blots were incubated with anti-phospho-GSK3β (Ser9), anti-phospho-MEK1/2 (Ser217/221), anti-MEK1/2, anti-phospho-ERK (Thr202/Tyr204), anti-ERK, anti-phospho-c-jun (Ser73), anti-phospho-c-fos (Ser32) at 1:1000 and anti-β-actin at 1:5000 (all antibodies were from Cell Signaling Technology). By incubating with the fluorescently labeled secondary antibodies for 1 h, the antibody-bound proteins were revealed by using the fluorescent Western-blot imaging systems (Odyssey).

For fractionation, cells were treated with TPA (200 ng/ml) or the vehicle control for 4 h prior to harvesting. 10^7 cells were lysed for 10 min on ice the cytoplasmic lysis buffer (10 mM Hepes at pH 8.0, 1.5 mM MgCl2, 10 mM KCl, 0.5 mM DTT, 300 mM sucrose, 0.1% NP-40, 10 mM NaF, 20 mM β-glycerophosphate, 10 mM Na_3VO_4, 1 × protease inhibitors, 0.5mMPMSF) for 10 min on ice and then quick-spun for 15 s to collect cytosolic lysate. In addition, 4×10^7 cells were lysed with nuclear lysis buffer (50 mM Hepes at pH 7.9, 250 mM KCl, 0.1 mM EDTA, 0.1 mM EGTA, 0.1% NP-40, 0.1% glycerol, 10 mM NaF, 10 mM Na3VO4, 1 mM DTT, 1 × protease inhibitors, 0.5 mM PMSF) for 30 min on ice. The lysates were spun for 20 min at 15,000 rpm at 4 °C to collect nuclear lysates. Lysates were then run in SDS-PAGE for Western blot analysis.

RNA isolation and real-time quantitative PCR (RT-qPCR)

Skin RNAs were isolated using the Trizol reagent (Invitrogen, USA). cDNAs were synthesized by using the M-MLV reverse transcriptase kit (Promega), and used as the templates for qPCR (MxPro QPCR Software) according to manufactural instructions. The following human primers were used: *GAPDH*: forward, 5′-ACCCAGAAGACTGTGGATGG-3′, reverse,5′-TTCAGCTCAGGGATGACCTT-3′; *Lgr4*: forward, 5′-

AAGATAACAGCCCCCAAGAC-3′, reverse, 5′-AGGCAGTGATGAACAAGACG-3′;*c-Myc*: forward,5′-TCCTGTACCTCGTCCGATTC-3′,,reverse, 5′-GGTTTGCCTCTTCTCCACAG-3′;*cyclinD1*: forward, 5′-GCGTACCCTGACACCAATCT-3′, reverse, 5′-CTCCTCTTCGCACTTCTGCT-3′.

The following mouse primers were used: *GAPDH*: forward, 5′-ACCCAGAAGACTGTGGATGG-3′, reverse,5′-TTCAGCTCAGGGATGACCTT-3′;*Lgr4*: forward, 5′-ACCTGGAGACCTTAGACTTG-3′, reverse 5′-CCACGAATGACTAGGGAATG-3;*c-Myc*: forward, 5′-GTCAAGAGGCGAACACACAAC-3′,reverse, 5′-TTGGACGGACAGGATGTATGC-3′ *Ccnd1*: forward, 5′-GTGGCCTCTAAGATGAAGGAGA-3′; reverse, 5′-GGAAGTGTTCAATGAAATCGTG-3′. The PCR condition was 95 °C for 3min followed by 40 cycles at 95 °C for 15 s, 60 °C for 30 s, and then 72 °C for 30 s.

Statistical analysis

All data are presented as mean ± SD. Student's t-test was performed to determine the statistical significance of differences between the groups. $p < 0.05$ was considered statistically significant.

Results

Lgr4 is crucial for DMBA/TPA-induced skin tumorigenesis in mice

To explore the function of Lgr4 in skin tumorigenesis, we followed DMBA-initiated and TPA-promoted two-stage chemical carcinogenesis protocol and compared tumor incidence and tumor multiplicity of WT and *Lgr4*-deficient mice. WT mice developed papillomas as early as 8 weeks after TPA treatment. By 12 weeks post-DMBA/TPA administration, 90% of the WT mice had developed papillomas. In contrast, of a total of 12 KO-mice examined, only 1 developed a tumor-like structure at 15 weeks after TPA treatment (Fig. 1a and b). On average, $Lgr4^{+/+}$ mice developed 5.02 tumors per mouse with 20 weeks of TPA treatment, whereas the average number of tumor-like structures formed per $Lgr4^{-/-}$ mouse is only 0.08 (Fig. 1c). The tumor-like structures in $Lgr4^{-/-}$ mice were also considerably smaller than the tumors in $Lgr4^{+/+}$ mice (Fig. 1d). All skin tumors derived from $Lgr4^{+/+}$ mice were well-differentiated squamous cell papillomas (Fig. 1e), albeit with different histopathological grades (Supplemental Fig. S1). In contrast, the tumor-like growths produced by the KO mice contained only a hyperproliferative epidermis (Fig. 1e). Thus, loss of Lgr4 renders the mice near-completely resistant to chemically induced skin tumorigenesis.

Lgr4 deficiency reduces TPA-dependent epidermal hyperplasia and keratinocyte proliferation

To understand the mechanism underlying the resistance to carcinogenesis in *Lgr4* KO mice, we examined the effects of short-term TPA treatment on epidermal cell proliferation. As shown in Fig. 2a, $Lgr4^{+/+}$mouse skin treated with TPA for one week or two weeks exhibited a marked increase in epidermal thickness compared with *Lgr4* KO mouse skin. The numbers of cells positive for proliferating cell nuclear antigen (PCNA) or for Ki67 was significantly

higher in *Lgr4* KO skin than that in the WT (Fig. 2b and c). Thus, the resistance to tumor formation in *Lgr4* KO mouse skin correlates with a decrease in epidermal cell proliferation.

To further determine the effects of Lgr4 on epidermal cell proliferation, we used a shRNA knockdown approach to deplete endogenous Lgr4 protein in A431 cells, a human epidermoid carcinoma cell line (Supplemental Fig. 2a and 2b). As shown in Fig. 3a, Lgr4 knockdown resulted in a dramatic reduction in cell number. Moreover, flow cytometric analysis revealed a significant reduction in the number of cells progressing through G1 (Fig. 3b). In addition, Lgr4 knockdown showed an approximate 50% reduction in cloning efficiency in soft agar when compared with control cells (Fig. 3c and d). Importantly, primary keratinocytes derived from *Lgr4* KO mice also showed decreased proliferation compared with their WT counterparts (Fig. 3e).

Resistance to tumorigenesis in Lgr4-deficient mice correlates with reduced MEK/ERK signaling

It is known that mice lacking epidermal Mek1 protein develop fewer papillomas than WT mice following DMBA/TPA treatment [9]. To address how Lgr4 affects skin keratinocyte proliferation, we measured the activity/level of MAPK pathway components. As shown in Fig. 4a, marked elevation of p-ERK1/2, p-c-fos and p-c-jun levels was observed in negative control shRNA (shNC) A431 cells after TPA treatment, whereas sh*Lgr4* cells were less responsive. Consistently, the extent of activation of MEK1/ERK/AP-1 in primary keratinocytes from $Lgr4^{-/-}$ was significantly lower than that in those from control littermates (Fig. 4b).

We next compared MEK/ERK pathway status in WT and *Lgr4* KO mice. The levels of phosphorylated MEK1 and ERK1/2 were significantly increased in WT mice following TPA treatment (Fig. 4c). The levels of AP-1 proteins (c-fos and c-jun) were also increased. In *Lgr4* KO mice, however, TPA treatment induced only a slight alteration in the levels of p-MEK1 and p-ERK1/2 (Fig. 4c). Together, our results indicate that Lgr4 deficiency compromises the TPA-induced activation of MEK1/ERK1/2 signaling both *in vitro* and *in vivo*.

Lgr4 is required for maximal Wnt/β-catenin signaling in skin cells

It has been shown that the β-catenin/TCF pathway is constitutively activated in non-melanocytic skin tumors in the two-stage chemical carcinogenesis model [13]. We thus investigated the relationship between Lgr4 and Wnt/β-catenin signaling in our model. As shown in Fig. 5a, primary keratinocytes derived from WT mice showed an obvious increase in the level of β-catenin protein after TPA treatment, whereas cells from *Lgr4* KO mice were insensitive to TPA in terms of β-catenin elevation. GSK3β is known to phosphorylate β-catenin and cause its degradation [22]. Phosphorylation of GSK3β on Ser9 blocks the interaction between GSK3β and β-catenin, thereby increasing β-catenin stability [23]. We therefore asked whether Lgr4 deletion affects β-catenin protein level by regulating Ser9 phosphorylation of GSK3β. Indeed, p-GSK3β (Ser9) level was greatly increased in keratinocytes from WT mice after TPA treatment, whereas the extent of increase was significantly reduced in *Lgr4* KO keratinocytes (Fig. 5a). Consistently, TPA treatment

markedly enhanced β-catenin and p-GSK3β (Ser9) levels in WT skin, but not in skin of *Lgr4* KO mice (Fig. 5b). Interestingly, even under physiological (untreated) conditions, the levels of β-catenin and p-GSK3β (Ser9) were slightly higher in WT skin than in *Lgr4* KO skin (Fig. 5b). Moreover, in A431 cells, TPA elicited an increase in β-catenin and p-GSK3β (Ser9) levels in a time-dependent manner, but this increase was not obvious when Lgr4 was depleted (Fig. 5c).

To further determine the effects of Lgr4 on β-catenin activity, we performed indirect immunofluorescence to examine β-catenin accumulation in primary keratinocytes. As expected, TPA treatment induced a more prominent nuclear accumulation of β-catenin in keratinocytes from WT mice than keratinocytes from the *Lgr4* KO mice (Fig. 5d and e). Similarly, TPA induced more obvious nuclear accumulation of β-catenin in shNC A431 cells than shLgr4 cells (Fig. 5f and g). These results demonstrate a cell-autonomous inhibition of Lgr4 deficiency on TPA-induced β-catenin accumulation in skin epidermal cells. Results of cell fractionation experiments corroborated this notion, as after TPA treatment, a higher increase in the level of nuclear β-catenin was detected in WT than *Lgr4* KO primary keratinocytes (Fig. 5h).

In addition, we examined the expression of β-catenin target genes by RT-qPCR. The levels of *Ccnd1* and *c-Myc* transcripts were considerably lower in *Lgr4* KO skin compared with WT skin, especially after TPA treatment (Fig. 5i). Consistently, the expression of *CCND1* and *c-MYC* was markedly increased in shNC A431 cells after TPA treatment compared with shLgr4 cells (Fig. 5j). Together, these *in vivo* and *in vitro* findings show a dependence of Wnt/β-catenin signaling output on Lgr4.

Both MEK/ERK and Wnt/β-catenin signaling contributes to skin cancer formation

Given that both ERK1/2 and β-catenin pathways were activated by TPA in WT skin, we wondered about their possible relationship. In WT mouse primary keratinocytes, ERK activation occurred at 4 h and peaked at 6 h after TPA treatment (Fig. 6a). The accumulation of β-catenin followed the same time course. In human SCC samples, higher expression of both p-ERK and β-catenin was observed compared with normal skin. Moreover, Lgr4 showed a positive correlation with both p-ERK and β-catenin in human SCC samples (Fig. 6b).

Next, we examined the interdependence of the two signaling pathways by using specific pathway inhibitors. As shown in Fig. 6c, MEK/ERK inhibitor U0126 significantly blocked TPA-induced ERK1/2 activation in primary keratinocytes derived from both WT and *Lgr4* KO mice. Interestingly, p-GSK3β and β-catenin were also markedly reduced in level by U0126. Moreover, TPA-induced increase in cyclin D1 protein was greatly inhibited by U0126 (Fig. 6c). Similar results were obtained in A431 cells upon *Lgr4* knockdown (Fig. 6d). On the other hand, although β-Catenin/TCF inhibitor FH535 effectively blocked the increase in cyclin D1 protein level, p-ERK level was not altered (Fig. 6c).

The above findings suggest a dependence of β-Catenin/TCF pathway activity on MEK/ERK signaling in epidermal cells. To further test this hypothesis, we next attempted to reduce the expression of ERK1/2 by using shRNA-expressing lentiviruses. Both shERK1 and shERK2

effectively reduced the levels of p-ERK1/2 in primary keratinocytes (Fig. 6e). Consistent with data described above, TPA treatment significantly increased p-ERK and β-catenin levels in primary keratinocytes. Depletion of ERK1/2 resulted in a marked reduction of β-catenin levels in these cells (Fig. 6e). Furthermore, both U0126 and FH535 inhibited the expression of cyclin D1 as well as TPA-induced proliferation of A431 cells (Fig. 6f). Taken together, these results show that MEK/ERK activation lies upstream of β-catenin signal pathway in normal and cancerous epidermal cells.

Discussion

Our work presents the detailed functional study on the involvement of Lgr4 in skin tumorigenesis. Specifically, we show that Lgr4 is required for papilloma formation in a two-stage skin carcinogenesis mouse model. Moreover, we provide both *in vitro* and *in vivo* evidences suggesting that Lgr4 likely does so by promoting TPA-induced keratinocyte proliferation and by regulating MAPK/ERK and Wnt/β-catenin signaling pathways.

The mitogen-induced ERK/MAPKs are linked to cell proliferation and survival [24]. ERK1 and ERK2 are activated by mitogens and are upregulated in several types of human tumors. Mutant BRAFV600E acts as a homodimer to drive consecutive ERK pathway activation, leading to the formation of melanoma, thyroid and colon cancer [25]. TPA can substitute for diacylglycerol (DAG) for activating protein kinase C (PKC) and is used as a classical skin tumor promoter. PKC is well known as an activator of the ERK pathway [26]. In WT mice, TPA treatment markedly increased the activation of MEK1 and ERK1/2, while it failed to do so in *Lgr4* KO mice. These results suggest that Lgr4 is required for TPA-induced MEK/ERK activation during skin tumor formation. Consistently, Wang et al. also found Lgr4 to mediate keratinocyte proliferation by increasing the phosphorylation of EGFR, ERK and STAT3 [27]. A mechanistic understanding of exactly how Lgr4 regulates the ERK pathway is still lacking and awaits future work that lies outside the scope of this study.

Several previous studies showed that Lgr4 plays an important role in multiple organ development processes and in promoting colon cancer cell proliferation/metastasis by activating Wnt signaling [18,20,28]. In the present study, we found that *Lgr4* deletion negatively impacts TPA-induced nuclear accumulation of β-catenin and expression of β-catenin target genes, raising the possibility that activation of β-catenin at least in part mediates the role of Lgr4 in accelerating skin tumor formation. A possible sequence of events in WT mice is that TPA stimulation upregulates ERK activity, which in turn leads to the phosphorylation of GSK3β and consequently increased Wnt/β-catenin pathway activity. Our data suggest that Lgr4 impinges on the early step(s) of this sequence. The function of Lgr4 in regulating both ERK and β-catenin signaling is reminiscent of that of its homolog, Lgr5, which has been shown to regulate pro-survival MEK/ERK signaling and proliferative Wnt/β-catenin signaling in neuroblastoma [29].

We found that ERK inhibitor and siRNA effectively suppressed TPA-induced increase in β-catenin, whereas a β-catenin/TCF inhibitor did not alter p-ERK level. These data suggest that activation of MEK/ERK signing lies upstream of activation of Wnt/β-catenin signaling during chemically induced skin tumorigenesis. In the absence of Lgr4, ERK is not

activated by TPA treatment and β-catenin activation is also compromised. These findings are consistent with a model where Lgr4 positively regulates Wnt/β-catenin signaling pathway during skin tumorigenesis in a manner that requires the activation of MEK/ERK signaling.

It is well known that the phosphorylation of β-catenin by GSK3β triggers its degradation. In our study, the levels of p-GSK3β (ser9) positively correlated with β-catenin accumulation after TPA treatment *in vitro* and *in vivo*. It has been reported that the ERK1/2 cascade is associated with phosphorylation of GSK3β at Ser9, resulting in inactivation of GSK3β and upregulation of β-catenin [30,31]. Thus, it seems plausible that TPA-induced activation of ERK in the skin of WT mice contributes to the phosphorylation of GSK3β and consequently β-catenin accumulation. AKT also has the potential to promote the phosphorylation of GSK3β at Ser9 [32]. However, we did not find any obvious change in p-AKT level in keratinocyte after TPA treatment.

Together, our study identifies Lgr4 as a critical promoting factor of skin carcinogenesis and a potential therapeutic target that may be explored in the future for skin cancer therapy. Heterozygous loss of *LGR4* in human is reported to be associated with increased risk of skin SCC [33], a finding that is in apparent conflict with our results. Towards verifying the role Lgr4 in human skin cancer, we examined its expression in human normal skin, SCC, basal cell carcinoma (BCC), and melanoma samples by immunohistochemical staining. Lgr4 protein was seen in the basal layer of normal skin, as well as in the basal layer-derived regions of early-stage SCC and BCC samples [Supplemental Fig. 3]. However, Lgr4 expression was barely detectable in the advanced cancer tissues of SCC and BCC. In human melanoma tissues, Lgr4 showed more positive staining than advanced SCC and BCC [Supplemental Fig. 3]. It is important to note that exposure to ultraviolet (UV) radiation is a major risk factor for most human skin cancers, and as such human skin carcinogenesis presents some differences from DMBA/TPA-induced skin carcinogenesis in the mouse model. Future studies are necessary to elucidate the detailed molecular mechanism of Lgr4 action in human SCC.

In conclusion, our data support a model in which Lgr4 promotes skin tumor formation in a DMBA/TPA animal model by activating MEK/ERK and Wnt/β-catenin signaling pathways. It seems that TPA stimulation upregulates ERK activity, leading to phosphorylation of GSK3 and increased activity of Wnt/β-catenin signaling in the WT mice (Fig. 7). In the absence of Lgr4, activation of MEK/ERK pathway, and consequently Wnt/β-catenin pathway, in response to TPA are blocked, leading to protection against skin tumor formation.

Supplementary Material

Refer to Web version on PubMed Central for supplementary material.

Acknowledgement

This work was supported by the grants from National Natural Science Foundation of China (No. 81272226, No. 81271742), the grants from the Key Science and Technology Projects from the Science and Technology Commission of Shanghai Municipality (13JC1405102, 13DZ1930906).

References

[1]. Mendive F, Laurent P, Van Schoore G, Skarnes W, Pochet R, Vassart G, Defective postnatal development of the male reproductive tract in Lgr4 knockout mice, Dev. Biol. 290 (2006) 421–434. [PubMed: 16406039]

[2]. Siwko S, Lai L, Weng J, Liu M, Lgr4 in ocular development and glaucoma, J. Ophthalmol. 2013 (2013) 987494. [PubMed: 23840940]

[3]. Mohri Y, Kato S, Umezawa A, Okuyama R, Nishimori K, Impaired hair placode formation with reduced expression of hair follicle-related genes in mice lacking Lgr4, Dev. Dyn. 237 (8) (2008) 2235–2242. [PubMed: 18651655]

[4]. Luo J, Zhou W, Zhou X, Li D, Weng J, Yi Z, et al. , Regulation of bone formation and remodeling by G-protein-coupled receptor 48, Development 136 (16) (2009) 2747–2756. [PubMed: 19605502]

[5]. Mazerbourg S, Bouley DM, Sudo S, Klein CA, Zhang JV, Kawamura K, et al. , Leucine-rich repeat-containing, G protein-coupled receptor 4 null mice exhibit intrauterine growth retardation associated with embryonic and perinatal lethality, Mol. Endocrinol. 18 (2004) 2241–2254. [PubMed: 15192078]

[6]. Liang F, Yue J, Wang J, Zhang L, Fan R, Zhang H, et al. , GPCR48/LGR4 promotes tumorigenesis of prostate cancer via PI3K/Akt signaling pathway, Med. Oncol. 32 (3) (2015) 49. [PubMed: 25636507]

[7]. Gao Y, Kitagawa K, Hiramatsu Y, Kikuchi H, Isobe T, Shimada M, et al. , Up-regulation of GPR48 induced by down-regulation of p27Kip1 enhances carcinoma cell invasiveness and metastasis, Cancer Res. 66 (24) (2006) 11623–11631. [PubMed: 17178856]

[8]. Kim EK, Choi EJ, Pathological roles of MAPK signaling pathways in human diseases, Biochim. Biophys. Acta 1802 (4) (2010) 396–405. [PubMed: 20079433]

[9]. Scholl FA, Dumesic PA, Barragan DI, Harada K, Charron J, Khavari PA, Selective role for Mek1 but not Mek2 in the induction of epidermal neoplasia, Cancer Res. 69 (9) (2009) 3772–3778. [PubMed: 19383924]

[10]. Wei Q, Jiang H, Matthews CP, Colburn NH, Sulfiredoxin is an AP-1 target gene that is required for transformation and shows elevated expression in human skin malignancies, Proc. Natl. Acad. Sci. U. S. A. 105 (50) (2008) 19738–19743. [PubMed: 19057013]

[11]. Cheepala SB, Yin W, Syed Z, Gill JN, McMillian A, Kleiner HE, et al. , Identification of the B-Raf/Mek/Erk MAP kinase pathway as a target for all-trans retinoic acid during skin cancer promotion, Mol. Cancer 8 (2009) 27. [PubMed: 19432991]

[12]. Clevers H, Nusse R, Wnt/β-catenin signaling and disease, Cell 149 (6) (2012) 1192–1205. [PubMed: 22682243]

[13]. Bhatia N, Spiegelman VS, Activation of Wnt/beta-catenin/Tcf signaling in mouse skin carcinogenesis, Mol. Carcinog. 42 (4) (2005) 213–221. [PubMed: 15765534]

[14]. Prasad R, Katiyar SK, Ultraviolet radiation-induced inflammation activates β-catenin signaling in mouse skin and skin tumors, Int. J. Oncol. 44 (4) (2014) 1199–1206. [PubMed: 24481495]

[15]. Li J, Ji L, Chen J, Zhang W, Ye Z, Wnt/β-catenin signaling Pathway in skin carcinogenesis and therapy, Biomed. Res. Int. 2015 (2015) 964842. [PubMed: 26078973]

[16]. de Lau W, Barker N, Low TY, Koo BK, Li VS, Teunissen H, et al. , Lgr5 homologues associate with Wnt receptors and mediate R-spondin signalling, Nature 476 (2011) 293–297. [PubMed: 21727895]

[17]. Glinka A, Dolde C, Kirsch N, Huang YL, Kazanskaya O, Ingelfinger D, et al. , LGR4 and LGR5 are R-spondin receptors mediating Wnt/β-catenin and Wnt/PCP signalling, EMBO Rep. 12 (10) (2011) 1055–1061. [PubMed: 21909076]

[18]. Wu J, Xie N, Xie K, Zeng J, Cheng L, Lei Y, et al. , GPR48, a poor prognostic factor, promotes tumor metastasis and activates β-catenin/TCF signaling in colorectal cancer, Carcinogenesis 34 (12) (2013) 2861–2869. [PubMed: 23803691]

[19]. Qian Y, Liu S, Guan Y, Pan H, Guan X, Qiu Z, et al. , Lgr4-mediated Wnt/β-catenin signaling in peritubularmyoid cells is essential for spermatogenesis, Development 140 (8) (2013) 1751–1761. [PubMed: 23533175]

[20]. Wang Y, Dong J, Li D, Lai L, Siwko S, Li Y, et al. , Lgr4 regulates mammary gland development and stem cell activity through the pluripotency transcription factor Sox2, Stem Cells 31 (9) (2013) 1921–1931. [PubMed: 23712846]

[21]. Liu S, Qian Y, Li L, Wei G, Guan Y, Pan H, et al. , Lgr4 gene deficiency increases susceptibility and severity of dextran sodium sulfate-induced inflammatory bowel disease in mice, J. Biol. Chem. 288 (13) (2013) 8794–8803. [PubMed: 23393138]

[22]. Xu W, Kimelman D, Mechanistic insights from structural studies of beta-catenin and its binding partners, J. Cell Sci. 120 (2007) 3337–3344. [PubMed: 17881495]

[23]. Garza JC, Guo M, Zhang W, Lu XY, Leptin restores adult hippocampal neurogenesis in a chronic unpredictable stress model of depression and reverses glucocorticoid-induced inhibition of GSK-3β/β-catenin signaling, Mol. Psychiatry 17 (8) (2012) 790–808. [PubMed: 22182938]

[24]. Boldt S, Weidle UH, Kolch W, The role of MAPK pathways in the action of chemotherapeutic drugs, Carcinogenesis 23 (11) (2002) 1831–1838. [PubMed: 12419831]

[25]. Cantwell-Dorris ER, O'Leary JJ, Sheils OM, BRAFV600E: implications for carcinogenesis and molecular therapy, Mol. Cancer Ther. 10 (3) (2011) 385–394. [PubMed: 21388974]

[26]. Ueda Y, Hirai Si, Osada Si, Suzuki A, Mizuno K, Ohno S, Protein kinase C activates the MEK-ERK pathway in a manner independent of Ras and dependent on Raf, J. Biol. Chem. 271 (38) (1996) 23512–23519. [PubMed: 8798560]

[27]. Wang Z, Jin C, Li H, Li C, Hou Q, Liu M, et al. , GPR48-Induced keratinocyte proliferation occurs through HB-EGF mediated EGFR transactivation, FEBS Lett. 584 (18) (2010) 4057–4062. [PubMed: 20732323]

[28]. Yu CY, Liang GB, Du P, Liu YH, Lgr4 promotes glioma cell proliferation through activation of Wnt signaling, Asian Pac J. Cancer Prev. 14 (8) (2013) 4907–4911. [PubMed: 24083766]

[29]. Vieira GC, Chockalingam S, Melegh Z, Greenhough A, Malik S, Szemes M, et al. , LGR5 regulates pro-survival MEK/ERK and proliferative Wnt/β-catenin signalling in neuroblastoma, Oncotarget 6 (37) (2015) 40053–40067. [PubMed: 26517508]

[30]. Sugden P, Markou T, Weiss S, Glycogen synthase kinase 3 as a convergence point in hypertropic signaling, Life Sci. (2007) SA216.

[31]. Ding Q, Xia W, Liu JC, Yang JY, Lee DF, Xia J, et al. , Erk associates with and primes GSK-3beta for its inactivation resulting in upregulation of beta-catenin, Mol. Cell 19 (2) (2005) 159–170. [PubMed: 16039586]

[32]. Fang D, Hawke D, Zheng Y, Xia Y, Meisenhelder J, Nika H, et al. , Phosphorylation of beta-catenin by AKT promotes beta-catenin transcriptional activity, J. Biol. Chem. 282 (15) (2007) 11221–11229. [PubMed: 17287208]

[33]. Styrkarsdottir U, Thorleifsson G, Sulem P, Gudbjartsson DF, Sigurdsson A, Jonasdottir A, et al. , Nonsense mutation in the LGR4 gene is associated with several human diseases and other traits, Nature 497 (7450) (2013) 517–520. [PubMed: 23644456]

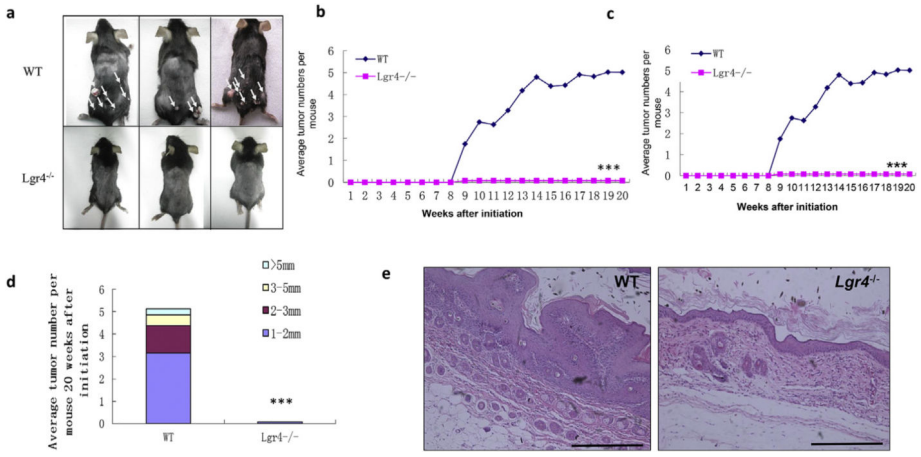

Fig. 1.

Lgr4 is critical for skin tumorigenesis in a mouse model. (a) Representative photographs of skin tumors showing the marked resistance to papilloma formation in *Lgr4*-deficient mice after 20 weeks of TPA promotion. (b) The percentage of tumor-bearing mice. (c) TPA-induced skin tumor numbers per mouse (two-tailed Student's test, n = 24 for *Lgr4* WT and KO mice, ***$p < 0.001$). (d) The average tumor volume/mouse (mm^3, two-tailed Student's test, n = 24 for Lgr4 WT and KO mice, ***$p < 0.001$). (e) Representative H&E staining of skin after 20 weeks of TPA promotion from WT and *Lgr4* KO mice. Scale bar, 100 μm (magnification, ×20).

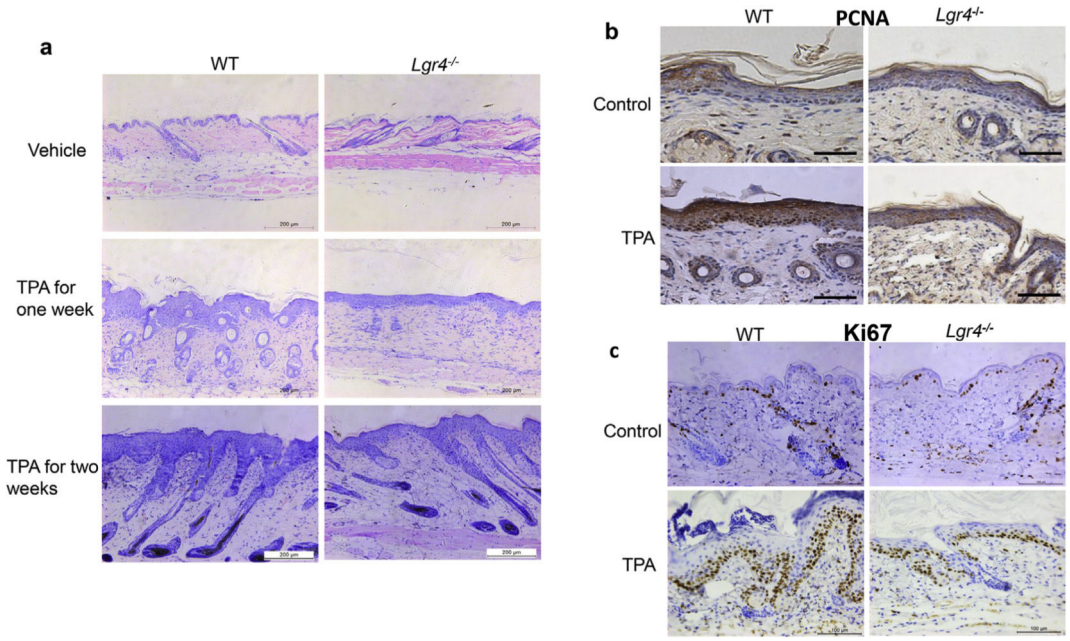

Fig. 2.

Epidermal hyperplasia in response to short-term TPA treatment. (a) H&E staining of dorsal skin from WT and *Lgr4* KO mice after TPA treatment for one or two weeks. Scale bar, 200 μm (magnification, ×10). (b) Immunohistochemical staining of PCNA in the skin from WT and *Lgr4* KO mice after TPA treatment for one week. Scale bar, 100 μm (magnification, ×20). (c) Immunohistochemical staining of Ki67 in the skin from WT and *Lgr4* KO mice after TPA treatment for two weeks. Scale bar, 200 μm (magnification, ×10).

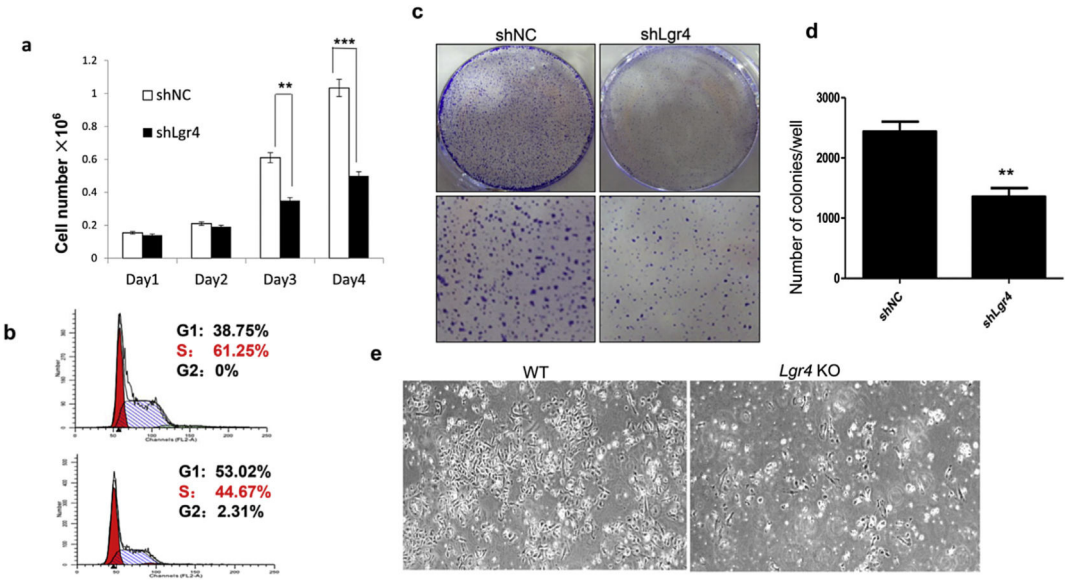

Fig. 3.

Knockdown of *Lgr4* inhibited skin cell proliferation. (a) Cell numbers of *Lgr4* knockdown and normal controls were counted every 24 h. Values are mean ± SD (n = 3). *p < 0.05, **p < 0.01. (b) Cell cycle analysis by flow cytometry. Knockdown of *Lgr4* by shRNA caused cell cycle arrest at G1 phase. (c) Soft agar colony formation assay. The clones of A431 cells were transferred to soft agar plates for incubation. After 2 weeks, the colony numbers were scored with a microscope and photographs were taken with a camera. (d) Colony numbers were counted in each well. Values are mean ± SD (n = 3). **p < 0.01. (e) Growth of primary keratinocyte isolated from *Lgr4* KO mice was slower than the WT counterparts. Representative images of WT and *Lgr4* KO colonies after culturing for 7 days. Scale bar, 100 μm (magnification, ×20).

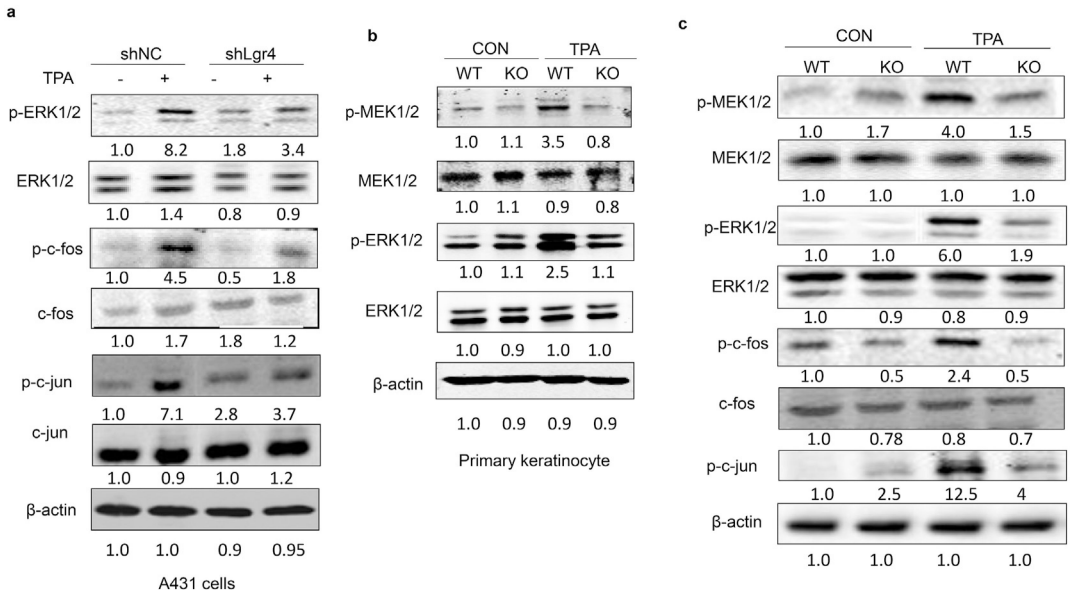

Fig. 4.

Lgr4 is required for TPA-induced activation of MEK/ERK signaling pathway in skin cancer. (a) Knockdown of *Lgr4* by shRNA attenuated the activation of MEK/ERK MAPK signaling induced by TPA. A431 cells were treated with or without TPA for 4 h, and cell lysates were subject to immunobloting analysis using the indicated antibodies. (b) *Lgr4* deletion inhibited TPA-induced activation of MEK/ERK signaling. Primary keratinocyte were treated with or without TPA for 4 h, and cell lysates were subject to immunobloting analysis. (c) Expression of MEK/ERK signaling molecules and downstream effector (AP-1) in WT and $Lgr4^{-/-}$ skin treated with TPA. Shown are results of immunoblot analysis of MEK, p-MEK, ERK, p-ERK, c-jun, p-c-jun, c-fos and p-c-fos.

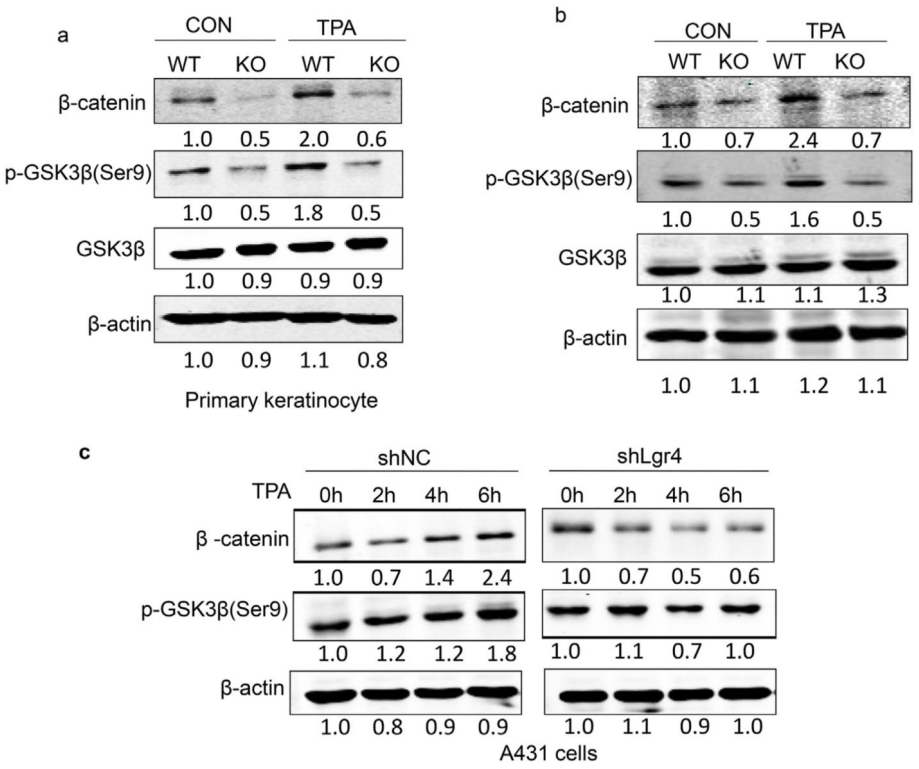

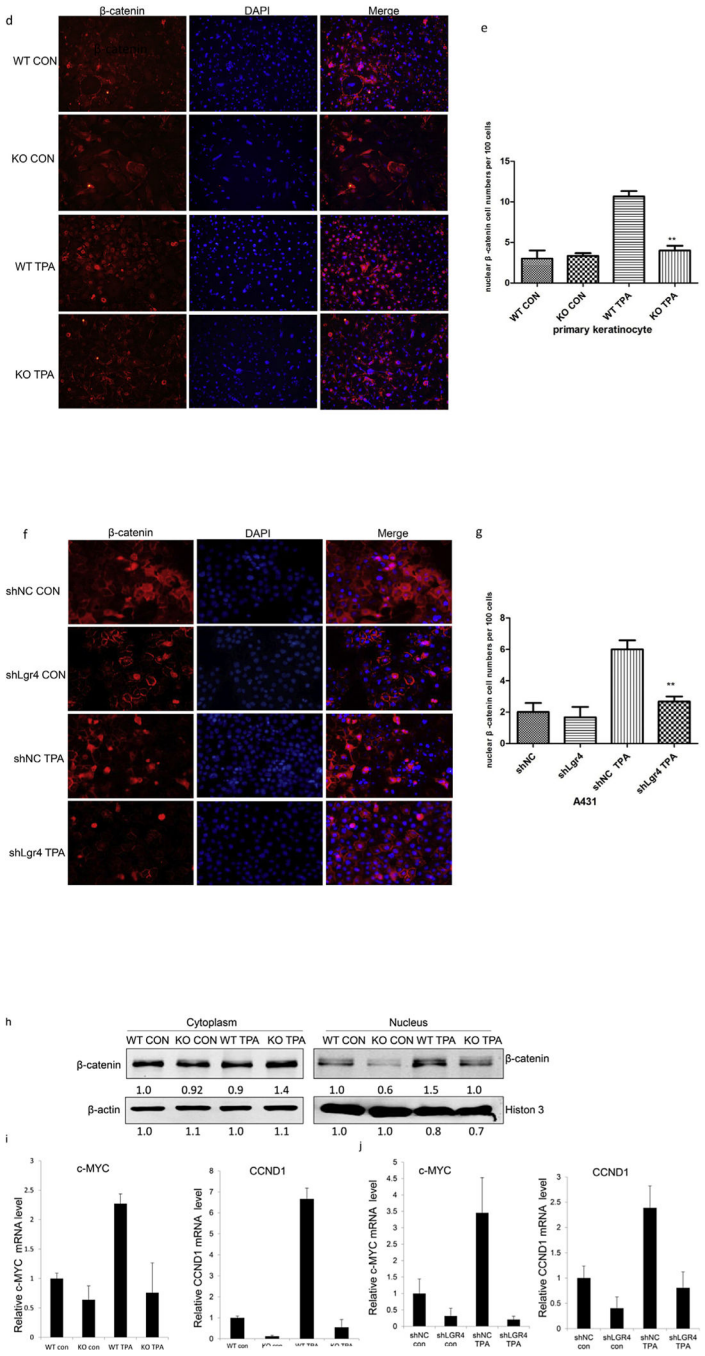

Fig. 5.

Lgr4 is required for TPA-induced changes in Wnt/β-catenin pathway components. (a) *Lgr4* deletion inhibited TPA-induced upregulation of β-catenin expression. Primary keratinocytes were treated with or without TPA for 4 h, and cell lysates were subject to immunobloting analysis. (b) Immunoblot analysis of β-catenin and p-GSK3β (Ser9) in the skin treated with or without TPA from WT and *Lgr4* KO mice. (c) Knockdown of *Lgr4* by shRNA inhibited the TPA-induced activation of Wnt/β-catenin signaling. A431 cells were treated with or without TPA for indicated time, and cell lysates were subject to immunobloting

analysis. (d) Immunofluorescence for β-catenin in primary keratinocytes treated with or without TPA for 4 h. Cells are counterstained with DAPI (blue). Scale bars, 100 μm. (e) Primary keratinocytes with β-catenin^{+} nuclei per group were quantified. Data are mean ± SD from three independent experiments; *$p < 0.05$, **$p < 0.01$. (f) Immunofluorescence for β-catenin in A431 cells treated with or without TPA for 4 h. Cells are counterstained with DAPI (blue). Scale bars, 100 μm. (g) A431 cells with β-catenin^{+} nuclei per group were quantified. The data were expressed as numbers of nuclear β-catenin per 100 cells from three independent experiments; *$p < 0.05$, **$p < 0.01$. (h) Primary keratinocytes treated with or without TPA for 4 h were fractionated into nuclear and cytoplasmic fractions, and 50 μg of protein for each fraction was analyzed by Western blotting for β-catenin, actin, and histon H3. Actin was used as a loading control, and histon H3 for purity of the nuclear fraction. (i) Quantitative RT-PCR analysis of *c-Myc* and *Ccnd1* in the skin treated with or without TPA from WT and *Lgr4* KO mice. (j) A431 cells were treated with or without TPA for 4 h, and cells were subjected to real-time PCR analysis for *c-Myc* and *Ccnd1*.

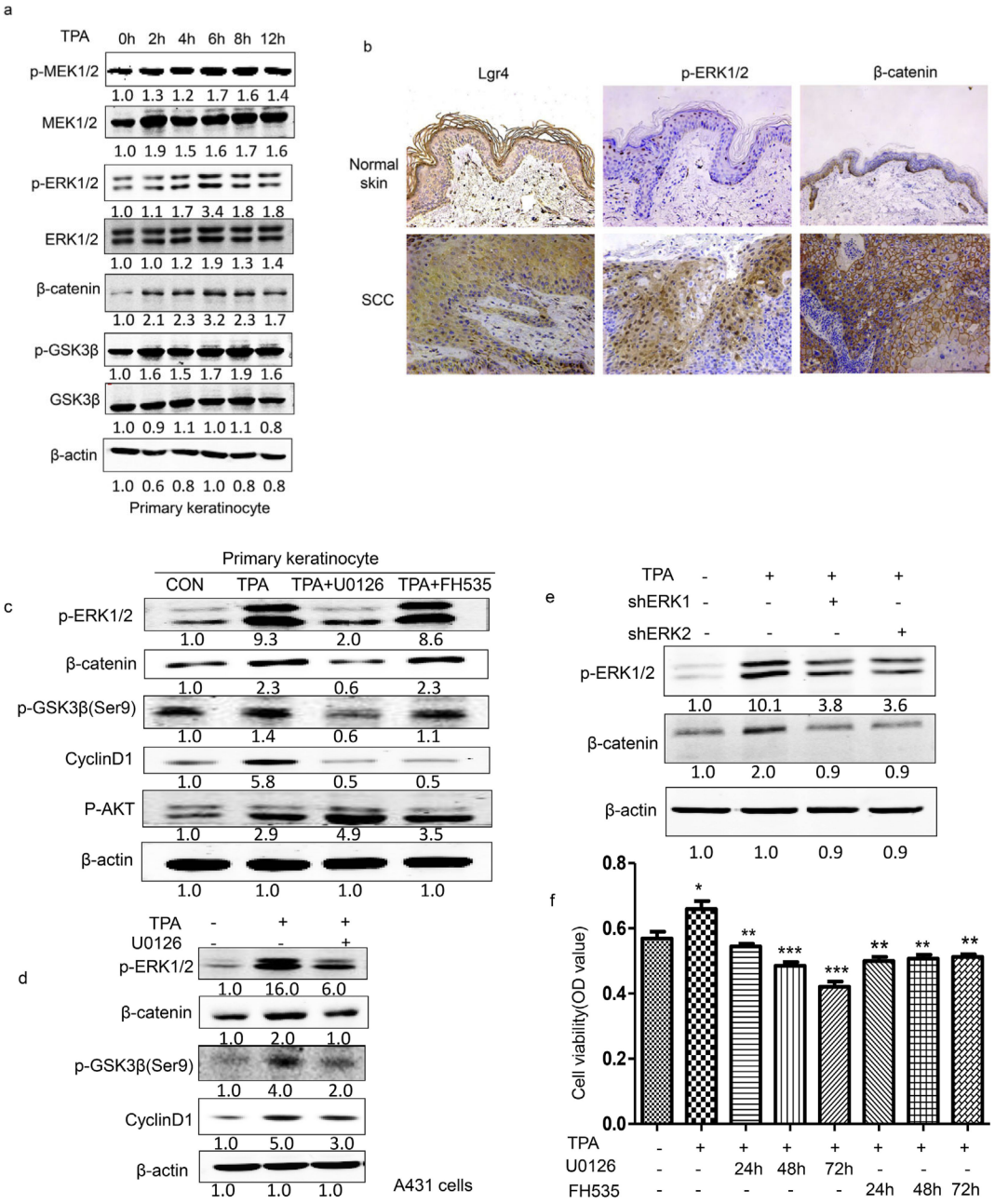

Fig. 6.

TPA-induced Wnt/β-catenin pathway component changes require MEK/ERK activity. (a) Primary keratinocyte were treated with or without TPA for the indicated time and cell lysates were subject to immunobloting analysis. (b) Immunohistochemical staining of Lgr4, p-ERK and β-catenin in human normal skin and SCC tissues. Scale bar, 200 μm (magnification, ×10). (c) Immunoblot analysis of p-ERK, p-GSK-3β, β-catenin and cyclin D1. Primary keratinocytes were treated with U0126 and FH535 for 30 m. (d) Immunoblot analysis of p-ERK, p-GSK-3β and β-catenin. A431 cells were treated with U0126 for 30 m. (e) Immunoblot analysis of p-ERK and β-catenin. (f) Inhibition of ERK or inhibition of β-catenin effectively reversed TPA-induced A431 cell proliferation. Cell viability was

analyzed by MTS every 24 h. Values are mean ± SD (n = 3). *p < 0.05, **p < 0.01, ***p < 0.001.

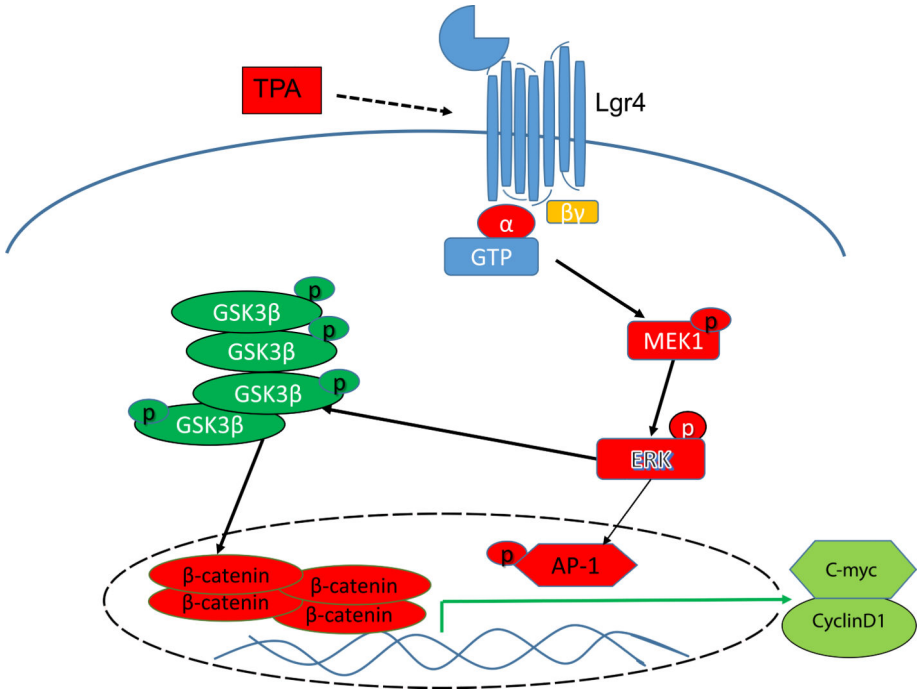

Fig. 7.

A proposed model for the role of Lgr4 in skin carcinogenesis. Lgr4 promotes skin tumor formation in a DMBA/TPA animal model by activating MEK/ERK and Wnt/β-catenin signaling pathways. In the skin of Lgr4 WT mice, TPA stimulation upregulates ERK activity, leading to phosphorylation of GSK3β and increased activity of Wnt/β-catenin signaling.